# Self-assembly of Polyoxometalate Conjugates: Novel Models for Catalytic Surfaces from Crystal Data†

**Mark P. Lowe, Joyce C. Lockhart,* George A. Forsyth, William Clegg and Kelly A. Fraser**
*Department of Chemistry, University of Newcastle, Newcastle upon Tyne NE1 7RU, UK*

Self-assembly of new organic conjugates of the pentamolybdodiphosphonato cage with cyclic aminomethylphosphonates has been achieved. The crystal structures of two of the conjugates have been determined and all of them characterised by IR spectroscopy. Intramolecular hydrogen bonding of the aminomethyl moiety to cage oxygen and close intermolecular C–H · · · O–Mo contacts (between 2.3 and 2.5 Å for the H · · · O distance) are observed, providing a new model for the interaction of substrates with a polyoxometalate catalytic surface. A scheme for modelling the pentamolybdodiphosphonato cage with a distance-restraint-based model is presented.

Self-assembly of biomolecules has a history as old as life; that of inorganic molecules is as old as geological time. While organic chemists are endeavouring to develop laboratory routes to self-assembly in a quest for supramolecular chemistry, equivalent self-assembly processes have been recognised by inorganic chemists for many years. Reuter[1] points out that inorganic host–guest compounds have been known since Berzelius[2] observed the formation of what was subsequently revealed to be the ammonium salt of 12-molybdophosphoric acid $[NH_4]_3[(PO_4)Mo_{12}O_{36}]$, a complex molecular structure generated from apparently simple molecular precursors. The important features to note are that the molybdate anions have the inherent ability to polymerise, the phosphate anion acts as a molecular template and the pH of the solution provides the chemical switch. In acidic media the assembly of the Keggin structure is facilitated, whereas in basic media the individual components exist as discrete molecules. In this paper we show how this inorganic mode of self-assembly can be used to drive assembly of *organic* moieties.

Of particular interest here are those derivatives incorporating phosphonic acid[3–6] moieties $RPO_3^{2-}$ (R = organic group) which introduce organic functionality into these predominantly inorganic assemblies. The formation of such structures has recently been investigated in solution by both $^{31}P$ NMR and electromotive force methods,[4,6–8] and in the solid state by infrared spectroscopy and X-ray crystallography.[3–5,9–12] Solution studies revealed several different species of heteropolyanion having varied P:Mo ratios and X-ray crystallographic data unequivocally confirm the existence of the conjugate $[(RP)_2Mo_5O_{21}]^{4-}$ anion; the structure has been solved for several phosphorus-containing species as well as for sulfur- and arsenic-containing conjugates. These structures can again, as with the Keggin-type anions, be self-assembled from their relatively uninteresting components on tripping the 'pH switch'.

Macrocycles with pendant aminomethylphosphonic acids have introduced a new field of chemistry into this already hybrid area of polymetalate–phosphorus chemistry, possessing the additional functionality required for the development of supramolecular chemistry,[13–15] while polyoxometalates with additional functionality are also in demand in materials sciences and other applications.[16–18] The conjunction of these two major areas of current research was recently achieved by the synthesis of the first examples of polyoxomolybdate cages derivatised with macrocycles, the crystal structure of conjugate **1** being solved.[6] The chemistry has now been extended further with cheap, readily available materials used in the synthesis of a range of conjugates and providing X-ray data on two more examples of the Strandberg[9] structure. The crystal structures are discussed and a force field for molecular modelling is developed.

**Table 1** Elemental analysis of conjugates **2–6** (calculated values in parentheses)

| Compound | *M* | Analysis (%) C | H | N |
|---|---|---|---|---|
| **2** | 1268.20 | 11.6 (11.4) | 2.8 (3.0) | 8.7 (8.8) |
| **3** | 1232.20 | 13.8 (13.7) | 3.4 (3.4) | 9.0 (9.1) |
| **4** | 1270.03 | 9.5 (9.4) | 2.9 (3.0) | 2.2 (2.2) |
| **5** | 1230.09 | 9.6 (9.8) | 2.2 (2.4) | 2.2 (2.3) |
| **6** | 1234.14 | 12.8 (12.7) | 3.3 (3.3) | 8.9 (9.1) |

## Experimental

Infrared spectra were recorded from KBr discs on a Nicolet 20PCIR spectrometer. Elemental analysis was obtained on a Carlo Erba 1106 Elemental Analyser.

*Synthesis.*—The general method for isolation of solid conjugates is similar[6] to that for conjugate **1** and is given in the following synthesis. The relevant pH values were generally chosen after observing the $^{31}P$ NMR spectra and noting where the concentration of the (*p*, 5,2) species ‡ is maximised. However when too low a pH was chosen, recrystallisation proved difficult and mixed precipitates were observed, probably containing guanidinium salts of isopolymolybdates, as well as the (*p*, 5,2) species, rather than the higher-ratio species which proved more soluble. Therefore the pH and recrystallisation conditions generally vary slightly. Analytical data are given in Table 1.

$[C(NH_2)_3]_2[\{S(CH_2CH_2)_2NHCH_2P\}_2Mo_5O_{21}]\cdot 2H_2O$, *conjugate* **2**. The salt $Na_2[MoO_4]\cdot 2H_2O$ (0.60 g, 2.50 mmol) and the monohydrate of thiomorpholinomethylphosphonic acid (0.21 g, 1.00 mmol) were dissolved with stirring in water (10

† *Supplementary data available:* see Instructions for Authors, *J. Chem. Soc., Dalton Trans.*, 1995, Issue 1, pp. xxv–xxx.

‡ The *p,q,r* notation is standard in polyoxometalate chemistry[5] and here refers to a conjugate with *p* protons, *q* molybdenums and *r* phosphonate residues.

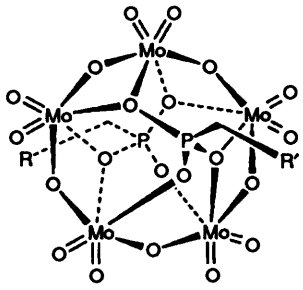

| Conjugate | | | |
|---|---|---|---|
| 1 | $[C(NH_2)_3]_2[(RCH_2P)_2Mo_5O_{21}]\cdot 3H_2O$ | R = R′ = | 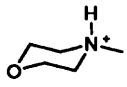 |
| 2 | $[C(NH_2)_3]_2[(RCH_2P)_2Mo_5O_{21}]\cdot 2H_2O$ | R = R′ = | 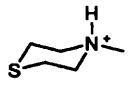 |
| 3 | $[C(NH_2)_3]_2[(RCH_2P)_2Mo_5O_{21}]\cdot 2H_2O$ | R = R′ = | 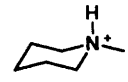 |
| 4 | $Na_2[(RCH_2P)_2Mo_5O_{21}]\cdot 8H_2O$ | R = R′ = | 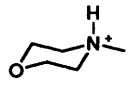 |
| 5 | $Na_2[(RCH_2P)_2Mo_5O_{21}]\cdot 4H_2O$ | R = R′ = | 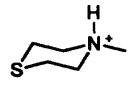 |
| 6 | $[C(NH_2)_3]_2[(RCH_2P)(R'CH_2P)Mo_5O_{21}]\cdot 2H_2O$ | R = | 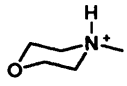 R′ = 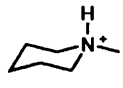 |

$cm^3$). Guanidinium carbonate (0.14 g, 0.78 mmol) was neutralised with 11.34 mol $dm^{-3}$ HCl and added dropwise to the stirred solution. The pH was reduced to 2.70 using 3 mol $dm^{-3}$ HCl. The white precipitate which formed was redissolved by heating the solution to 90 °C. The solution was cooled slowly to 70 °C and then maintained at this temperature for 3 d. Large colourless crystals formed (which turned dark red on excessive exposure to sunlight). Yield: 0.25 g, 40%.

$[C(NH_2)_3]_2[\{CH_2(CH_2CH_2)_2NHCH_2P\}_2Mo_5O_{21}]\cdot 2H_2O$, *conjugate* **3**. Colourless crystals prepared as for conjugate **2** were grown at pH 3.50 from a solution of $Na_2[MoO_4]\cdot 2H_2O$ (0.15 g, 0.62 mmol) and the monohydrate of piperidinomethylphosphonic acid (0.05 g, 0.25 mmol), guanidinium carbonate (0.04 g, 0.22 mmol) and water (10 $cm^3$). Yield: 0.08 g, 50%.

$Na_2[\{O(CH_2CH_2)_2NHCH_2P\}_2Mo_5O_{21}]\cdot 8H_2O$, *conjugate* **4**. This was prepared as for conjugate **2** at pH 3.0: large rectangular colourless crystals were obtained from a solution of $Na_2[MoO_4]\cdot 2H_2O$ (0.60 g, 2.50 mmol) and the monohydrate of morpholinomethylphosphonic acid (0.20 g, 1.00 mmol), NaCl (0.50 g, 8.50 mmol) and water (10 $cm^3$). Yield: 0.17 g, 27%.

$Na_2[\{S(CH_2CH_2)_2NHCH_2P\}_2Mo_5O_{21}]\cdot 4H_2O$, *conjugate* **5**. This was prepared as for conjugate **2** at pH 3.5: fine feathery crystals were obtained from a solution of $Na_2[MoO_4]\cdot 2H_2O$ (0.60 g, 2.50 mmol) and the monohydrate of thiomorpholinomethylphosphonic acid (0.21 g, 1.00 mmol), NaCl (0.60 g, 10.23 mmol) and water (10 $cm^3$). Yield: 0.09 g, 15%.

$[C(NH_2)_3]_2[\{O(CH_2CH_2)_2NHCH_2P\}\{CH_2(CH_2CH_2)_2NHCH_2P\}Mo_5O_{21}]\cdot 2H_2O$ **6**. This was prepared as for conjugate **2** at pH 3.5: small cubic crystals were separated from a needle-like precipitate from a solution of $Na_2[MoO_4]\cdot 2H_2O$ (0.60 g, 2.50 mmol), the monohydrate of morpholinomethylphosphonic acid (0.10 g, 0.50 mmol) and the monohydrate of piperidinomethylphosphonic acid (0.11 g, 0.50 mmol), NaCl (0.60 g, 10.23 mmol) and water (10 $cm^3$). Yield: 0.06 g, 10%.

*X-Ray Crystallography*.—Crystal data for conjugates 2 and 3 are given in Table 2, together with other information on the structure-determination procedures. Space group *I*2/*a* is a non-standard setting of *C*2/*c*, selected to avoid an unduly large value of the β angle. All measurements were made on a Stoe-Siemens diffractometer with graphite-monochromated Mo-Kα radiation (λ = 0.710 73 Å), at 160 K.[19] Cell parameters were refined from 2θ values (20–25°) for 31 or 32 reflections measured at ±ω to minimise systematic errors. Intensities were measured with ω–θ scans and on-line profile fitting[20] to $2\theta_{max} = 50°$. Each data set consisted of a complete unique quadrant of data, together with a partial set of symmetry-equivalent reflections. Corrections were made for slight decay (*ca.* 1% overall) of selected standard reflections measured periodically. Semiempirical absorption corrections were applied, based on sets of equivalent reflections measured at a range of azimuthal angles.[21] The structures were determined by direct methods and refined[21] by least squares on $F^2$ for all independent reflections in each case. A riding model was used for isotropic hydrogen atoms, except for the freely refined NH groups, and all other atoms were refined anisotropically. The weighting scheme was of the form $w^{-1} = \sigma^2(F_o^2) + (aP)^2 + bP$, where $P = (F_o + 2F_c)/3$. The extinction correction multiplies $F_c$ by the factor $(1 + 0.001xF_c^2\lambda^3/\sin 2\theta)^{-\frac{1}{4}}$, where $x$ is a refined isotropic extinction coefficient. Refined atomic coordinates are given in Tables 3 and 4, selected bond lengths and angles in Table 5. The anions are shown in Figs. 1 and 2, and a packing diagram in Fig. 3.

*Molecular Modelling*.—We used a method similar to that used for carborane cages.[22] The software available was

**Table 2** Crystallographic data

| Compound | 2 | 3 |
|---|---|---|
| Formula | $C_{12}H_{38}Mo_5N_8O_{23}P_2S_2$ | $C_{14}H_{42}Mo_5N_8O_{23}P_2$ |
| $M$ | 1268.3 | 1232.2 |
| Crystal system | Monoclinic | Monoclinic |
| Space group | $C2/c$ | $I2/a$ |
| $a$/Å | 20.727(8) | 20.606(3) |
| $b$/Å | 12.559(6) | 11.127(2) |
| $c$/Å | 16.082(7) | 16.348(3) |
| β/° | 118.77(4) | 101.58(5) |
| $U$/Å$^3$ | 3669(3) | 3672.0(11) |
| $Z$ | 4 | 4 |
| $D_c$/g cm$^{-3}$ | 2.296 | 2.229 |
| μ/mm$^{-1}$ | 1.957 | 1.842 |
| $F$(000) | 2488 | 2424 |
| Crystal size/mm | 0.54 × 0.42 × 0.32 | 0.50 × 0.31 × 0.17 |
| Reflections measured | 3878 | 5226 |
| Unique reflections | 3231 | 3232 |
| Reflections with $F^2 > 2\sigma(F^2)$ | 3001 | 3032 |
| $R_{int}$ | 0.0326 | 0.0314 |
| Transmission | 0.535–0.565 | 0.845–0.976 |
| No. of refined parameters | 246 | 246 |
| Weighting parameters $a,b$ | 0.0141, 19.7571 | 0.0139, 9.2473 |
| Extinction coefficient $x$ | 0.000 31(3) | 0.000 17(2) |
| $R$ (on $F$, observed data) | 0.0216 | 0.0183 |
| $R' = [\Sigma w(F_o^2 - F_c^2)^2/\Sigma w(F_o^2)^2]^{\frac{1}{2}}$ | 0.0912 | 0.0490 |
| Goodness of fit | 1.164 | 1.086 |
| Maximum shift/e.s.d. | 0.001 | 0.002 |
| Maximum, minimum electron density/e Å$^{-3}$ | 0.476, −0.445 | 0.431, −0.434 |

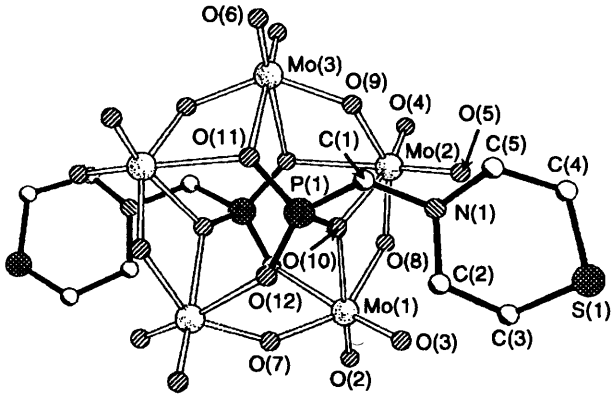


**Fig. 1** Crystal structure of conjugate **2**

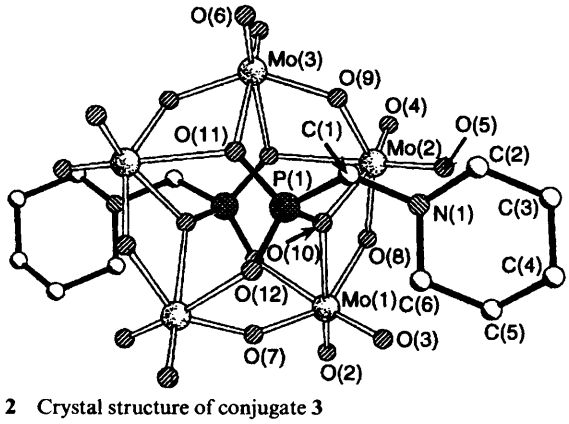


**Fig. 2** Crystal structure of conjugate **3**

**Table 3** Atomic coordinates ( × 10$^4$) for compound **2**

| Atom | $x$ | $y$ | $z$ |
|---|---|---|---|
| Mo(1) | 897.6(2) | −1358.5(2) | 2518.4(2) |
| Mo(2) | 1437.2(2) | 1206.8(2) | 2870.3(2) |
| Mo(3) | 0 | 2807.2(3) | 2500 |
| P(1) | 332.8(4) | 421.2(6) | 3813.7(5) |
| O(2) | 994.3(13) | −2276(2) | 1800(2) |
| O(3) | 1515.7(13) | −1777(2) | 3626(2) |
| O(4) | 1700.0(13) | 1981(2) | 2218(2) |
| O(5) | 2214.2(12) | 1092(2) | 3975(2) |
| O(6) | −111.6(13) | 3649(2) | 3255(2) |
| O(7) | 0 | −1805(2) | 2500 |
| O(8) | 1421.3(12) | −161(2) | 2353(2) |
| O(9) | 961.8(12) | 2275(2) | 3262(2) |
| O(10) | 778.0(12) | 158(2) | 3298(2) |
| O(11) | −216.3(12) | 1340(2) | 3349(2) |
| O(12) | −29.1(12) | −584(2) | 3900(2) |
| N(1) | 1762(2) | 487(2) | 5341(2) |
| C(1) | 1001(2) | 938(3) | 4972(2) |
| C(2) | 1779(2) | −681(3) | 5555(2) |
| C(3) | 2522(2) | −1182(3) | 5849(3) |
| S(1) | 3251.0(5) | −608.3(7) | 6922.1(7) |
| C(4) | 3085(2) | 752(3) | 6517(3) |
| C(5) | 2303(2) | 1115(3) | 6189(2) |
| C(6) | −578(2) | −3538(3) | 92(3) |
| N(2) | −755(2) | −4274(3) | −556(3) |
| N(3) | −444(2) | −2555(3) | −79(2) |
| N(4) | −523(3) | −3769(4) | 929(3) |
| O(1W) | 3715(2) | 1361(2) | 4437(2) |

**Table 4** Atomic coordinates ( × 10$^4$) for compound **3**

| Atom | $x$ | $y$ | $z$ |
|---|---|---|---|
| Mo(1) | 3 290.23(10) | 9 185.2(2) | 5 775.96(12) |
| Mo(2) | 3 807.99(10) | 6 288.9(2) | 5 856.23(12) |
| Mo(3) | 2 500 | 4 495.1(3) | 5 000 |
| P(1) | 2 816.3(3) | 7 139.1(6) | 3 995.4(4) |
| O(2) | 3 335.7(9) | 10 197(2) | 6 567.3(11) |
| O(3) | 3 863.9(9) | 9 712(2) | 5 243.9(11) |
| O(4) | 4 037.4(9) | 5 455(2) | 6 737.1(11) |
| O(5) | 4 510.4(8) | 6 398(2) | 5 431.2(11) |
| O(6) | 2 425.6(9) | 3 557(2) | 4 158.3(12) |
| O(7) | 2 500 | 9 628(2) | 5 000 |
| O(8) | 3 771.7(8) | 7 824(2) | 6 349.5(10) |
| O(9) | 3 391.3(8) | 5 037(2) | 5 082.1(10) |
| O(10) | 3 221.2(8) | 7 449(2) | 4 866.7(10) |
| O(11) | 2 321.4(8) | 6 110(2) | 4 017.9(10) |
| O(12) | 2 486.8(8) | 8 260(2) | 3 587.6(10) |
| N(1) | 4 091.7(10) | 7 090(2) | 3 675.3(13) |
| C(1) | 3 415.5(11) | 6 561(2) | 3 400(2) |
| C(2) | 4 582.7(12) | 6 455(2) | 3 248(2) |
| C(3) | 5 273.8(13) | 6 985(3) | 3 535(2) |
| C(4) | 5 276.7(14) | 8 329(3) | 3 374(2) |
| C(5) | 4 779.1(14) | 8 954(3) | 3 807(2) |
| C(6) | 4 092.0(13) | 8 424(2) | 3 527(2) |
| C(7) | 3 171.7(13) | 1 338(2) | 2 983(2) |
| N(2) | 3 337.8(11) | 2 245(2) | 2 536(2) |
| N(3) | 3 327(2) | 1 388(2) | 3 806(2) |
| N(4) | 2 854.7(11) | 396(2) | 2 608.4(14) |
| O(1W) | 4 062.8(11) | 3 659(2) | 4 081.9(13) |

QUANTA [23] which uses the CHARMm force field[24] (version 21.3) supplied by Polygen, and running on SG IRIS 4D20G machines. Since this force field contained only van der Waals parameters for molybdenum, a provisional set of distance restraints and force-field parameters, designed to reproduce the geometry of the cages as determined in the crystal structures, was added as follows: consensus geometries required were taken from the preceding crystallographic studies and the EPSRC CDS implementation (Daresbury) of the Cambridge Structural Database.[25] Distance restraints were used to replicate the cage

**Table 5** Selected bond lengths (Å) and angles (°) for the anions of compounds **2** and **3**

| | 2 | 3 | | 2 | 3 |
|---|---|---|---|---|---|
| Mo(1)–O(3) | 1.701(2) | 1.706(2) | Mo(2)–O(10) | 2.231(2) | 2.227(2) |
| Mo(1)–O(2) | 1.710(2) | 1.703(2) | Mo(2)–O(11a) | 2.345(3) | 2.385(2) |
| Mo(1)–O(7) | 1.9298(12) | 1.9169(12) | Mo(3)–O(6) | 1.708(2) | 1.709(2) |
| Mo(1)–O(8) | 1.946(2) | 1.945(2) | Mo(3)–O(9) | 1.890(2) | 1.912(2) |
| Mo(1)–O(12a) | 2.332(3) | 2.318(2) | Mo(3)–O(11) | 2.460(2) | 2.388(2) |
| Mo(1)–O(10) | 2.358(2) | 2.425(2) | P(1)–O(12) | 1.508(2) | 1.510(2) |
| Mo(2)–O(4) | 1.701(2) | 1.698(2) | P(1)–O(11) | 1.539(2) | 1.538(2) |
| Mo(2)–O(5) | 1.737(3) | 1.731(2) | P(1)–O(10) | 1.545(2) | 1.539(2) |
| Mo(2)–O(8) | 1.903(2) | 1.897(2) | P(1)–C(1) | 1.823(3) | 1.835(2) |
| Mo(2)–O(9) | 1.940(2) | 1.960(2) | | | |
| O(3)–Mo(1)–O(2) | 103.02(12) | 102.83(9) | O(9)–Mo(2)–O(11a) | 73.14(9) | 71.81(7) |
| O(3)–Mo(1)–O(7) | 99.26(10) | 99.08(7) | O(10)–Mo(2)–O(11a) | 74.07(8) | 73.40(7) |
| O(2)–Mo(1)–O(7) | 102.67(11) | 104.03(9) | O(6)–Mo(3)–O(6a) | 103.5(2) | 104.73(13) |
| O(3)–Mo(1)–O(8) | 101.15(11) | 100.06(8) | O(6)–Mo(3)–O(9a) | 102.61(11) | 101.92(9) |
| O(2)–Mo(1)–O(8) | 100.01(11) | 101.75(9) | O(6)–Mo(3)–O(9) | 102.69(11) | 100.30(9) |
| O(7)–Mo(1)–O(8) | 145.03(11) | 143.38(9) | O(9a)–Mo(3)–O(9) | 138.58(14) | 143.22(11) |
| O(3)–Mo(1)–O(12a) | 172.27(10) | 173.23(8) | O(6)–Mo(3)–O(11) | 86.88(10) | 86.64(8) |
| O(2)–Mo(1)–O(12a) | 84.66(10) | 83.71(8) | O(6a)–Mo(3)–O(11) | 169.05(10) | 167.79(7) |
| O(7)–Mo(1)–O(12a) | 79.72(8) | 80.78(6) | O(9a)–Mo(3)–O(11) | 71.20(9) | 72.50(7) |
| O(8)–Mo(1)–O(12a) | 76.26(9) | 76.66(7) | O(9)–Mo(3)–O(11) | 78.02(9) | 79.99(8) |
| O(3)–Mo(1)–O(10) | 84.94(10) | 85.55(8) | O(11)–Mo(3)–O(11a) | 82.98(11) | 82.43(8) |
| O(2)–Mo(1)–O(10) | 168.45(9) | 168.51(7) | O(12)–P(1)–O(11) | 112.82(13) | 112.57(10) |
| O(7)–Mo(1)–O(10) | 84.01(10) | 82.06(8) | O(12)–P(1)–O(10) | 108.82(13) | 109.65(10) |
| O(8)–Mo(1)–O(10) | 69.93(9) | 68.68(7) | O(11)–P(1)–O(10) | 113.14(13) | 112.54(10) |
| O(12a)–Mo(1)–O(10) | 87.33(8) | 87.73(6) | O(12)–P(1)–C(1) | 111.78(14) | 110.26(11) |
| O(4)–Mo(2)–O(5) | 105.33(11) | 105.41(9) | O(11)–P(1)–C(1) | 104.45(14) | 105.75(11) |
| O(4)–Mo(2)–O(8) | 100.92(11) | 99.17(8) | O(10)–P(1)–C(1) | 105.56(14) | 105.77(10) |
| O(5)–Mo(2)–O(8) | 100.65(11) | 102.42(8) | Mo(1a)–O(7)–Mo(1) | 146.2(2) | 150.2(2) |
| O(4)–Mo(2)–O(9) | 99.70(11) | 99.83(9) | Mo(2)–O(8)–Mo(1) | 122.08(11) | 123.79(9) |
| O(5)–Mo(2)–O(9) | 95.23(11) | 94.81(8) | Mo(3)–O(9)–Mo(2) | 125.19(12) | 124.03(9) |
| O(8)–Mo(2)–O(9) | 149.53(9) | 149.86(7) | P(1)–O(10)–Mo(2) | 130.71(13) | 131.10(11) |
| O(4)–Mo(2)–O(10) | 162.33(10) | 161.92(7) | P(1)–O(10)–Mo(1) | 134.50(13) | 134.45(10) |
| O(5)–Mo(2)–O(10) | 92.26(10) | 92.50(8) | Mo(2)–O(10)–Mo(1) | 94.39(8) | 93.44(6) |
| O(8)–Mo(2)–O(10) | 73.59(9) | 74.04(7) | P(1)–O(11)–Mo(2a) | 126.92(13) | 127.04(10) |
| O(9)–Mo(2)–O(10) | 79.99(9) | 80.74(8) | P(1)–O(11)–Mo(3) | 122.79(12) | 124.23(10) |
| O(4)–Mo(2)–O(11a) | 88.87(10) | 89.51(8) | Mo(2a)–O(11)–Mo(3) | 90.05(8) | 91.50(6) |
| O(5)–Mo(2)–O(11a) | 163.19(9) | 161.69(7) | P(1)–O(12)–Mo(1a) | 116.33(12) | 117.30(9) |
| O(8)–Mo(2)–O(11a) | 85.07(9) | 85.19(7) | | | |

Symmetry transformations used to generate equivalent atoms: a $-x, y, -z + \frac{1}{2}$ for compound **2**, $-x + \frac{1}{2}, y, -z + 1$ for **3**.

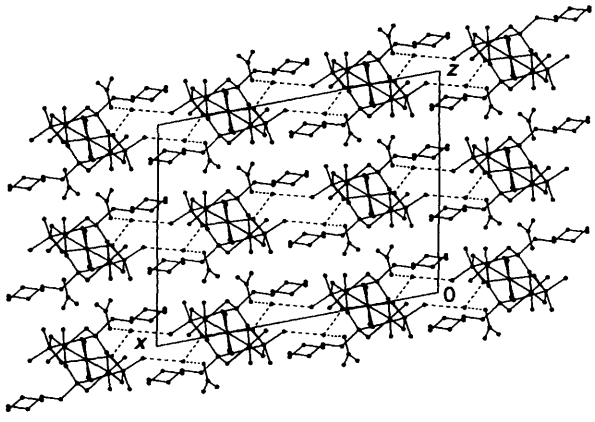


**Fig. 3** Packing of conjugate **3**, showing the intermolecular OH···O and NH···O hydrogen bonding. For clarity, hydrogen atoms, C–H···O and intramolecular hydrogen bonding are not shown. The view is along the crystallographic *b* axis

**Table 6** Assignment of atom types for CHARMm for the polyoxomolybdate cage[a]

| Atom type[b] | Atoms[c] | Description |
|---|---|---|
| MO1 | Mo(1), Mo(1a) | Equivalent molybdenums |
| MO2 | Mo(2), Mo(2a) | Equivalent molybdenums |
| MO3 | Mo(3) | Unique molybdenum |
| OA1 | O(2), O(2a), O(4), O(4a), O(6) | Terminal oxygens |
| OA2 | O(3), O(3a), O(5), O(5a), O(6a) | Terminal oxygens |
| OB | O(7), O(8), O(8a), O(9), O(9a) | Attached to two Mo |
| OC1 | O(12), O(12a) | Attached to Mo(1)/Mo(1a) and P |
| OC2A | O(11) | Attached to Mo(2a), Mo(3) and P |
| OC2B | O(11a) | Attached to Mo(2), Mo(3) and P |
| OC3 | O(10), O(10a) | Attached to Mo(1), Mo(2)/Mo(1a), Mo(2a) and P |

[a] Two conventions for labelling are used: one for crystal structures, and one for atom types for molecular modelling. [b] Atom types used for the CHARMm force field. [c] Labelled as in Figs. 1 and 2.

geometry while the associated Mo=O bonds and angles and non-cage atoms were described using CHARMm force-field parameters. The charges used were determined within CHARMm. The effect of varying the charge on the cage will be an interesting future study, but the values used (Mo, +1.07; O, −0.48) were consistent with those obtained by *ab initio* methods.[26]

*Atom types.* Atom types and numbers are shown in Table 6 based on the numbering scheme shown in Fig. 4. The distances used in the restraints were consensus ones defined for the average bond lengths and interatomic distances from the crystallographic sources. Seven different Mo–O bond types can be identified for the cage and 'consensus' bond lengths defined for these based on average bond lengths from crystallographic

**Table 7** Bonded distance restraints used in CHARMm for polyoxometalate cage

| | Distance (Å) | | Distance (Å) |
|---|---|---|---|
| Mo(1)–O(7) | 1.93 | Mo(1a)–O(7) | 1.93 |
| Mo(1)–O(8) | 1.93 | Mo(1a)–O(8a) | 1.93 |
| Mo(2)–O(8) | 1.93 | Mo(2a)–O(8a) | 1.93 |
| Mo(2)–O(9) | 1.93 | Mo(2a)–O(9a) | 1.93 |
| Mo(3)–O(9) | 1.93 | Mo(3)–O(9a) | 1.93 |
| Mo(1)–O(10) | 2.37 | Mo(1a)–O(10a) | 2.37 |
| Mo(2)–O(11a) | 2.37 | Mo(2a)–O(11a) | 2.37 |
| Mo(3)–O(11) | 2.37 | Mo(3)–O(11a) | 2.37 |
| Mo(1)–O(12a) | 2.29 | Mo(1a)–O(12) | 2.29 |
| Mo(2)–O(10) | 2.22 | Mo(2a)–O(10a) | 2.22 |
| P(1)–O(10) | 1.53 | P(1a)–O(10a) | 1.53 |
| P(1)–O(11) | 1.53 | P(1a)–O(11a) | 1.53 |
| P(1)–O(12) | 1.53 | P(1a)–O(12a) | 1.53 |

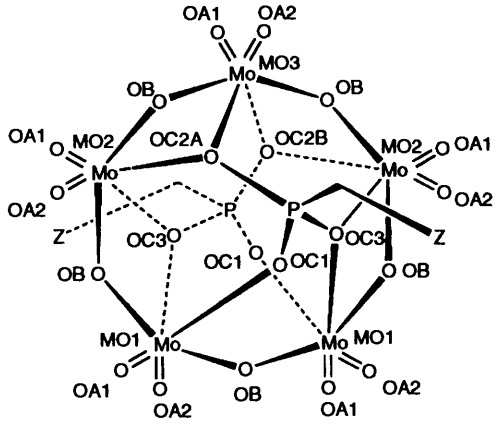


**Fig. 4** Atom labelling in pentamolybdodiphosphonato cages

sources. In general the cage dimensions are reproducible from one crystal structure to another. The restraints forces for the cages described in this work were applied according to equations (1)–(3). The energy term within CHARMm for a

$$E = k(r - r_0)^2 \quad (1)$$

$$k = 0.5Sk_bT/(r - r_0)^2 \quad (2)$$

$$k = 0.5Sk_bT/(r_0 - r)^2 \quad (3)$$

restraint to keep two atoms A and B within a certain distance of each other takes the form of equation (1) where $r$ is the distance between atoms A and B and $r_0$ is the restraint distance. The force constant ($k$) is defined in equations (2) and (3) for $r > r_0$ and $r < r_0$ respectively, where $k_b$ is the Boltzmann constant, $T$ the temperature (Kelvin), and $S$ the scaling factor, usually unity. At distance $r_0$ the value of the restraint energy is $0.5Sk_bT$. The restraint distances for the cage and the geometries used for the terminal oxygens (not included in distance restraints) were those given in Tables 7–9. The value used for $|r_0 - r|$ for the simulations reported was 0.02 Å. These simulations were for molecules *in vacuo*.

*Calibration.* The restraints were tested against known geometries and gave fits for the polyoxometalate cage exemplified in Fig. 5, with the total root-mean-square (r.m.s.) deviations shown in Table 10. In each case a rigid-body fit as described in the QUANTA manual was used for comparison.

## Results and Discussion

A series of new pentamolybdodiphosphonato cages bearing heterocyclic moieties was synthesised. The crystal structures of two such conjugates were elucidated; the structure of a third conjugate was reported previously.[6]

**Table 8** Non-bonded distance restraints used in CHARMm for polyoxometalate cage

| | Distance (Å) | | Distance (Å) |
|---|---|---|---|
| P(1)···P(1a) | 3.76 | | |
| Mo(1)···Mo(2a) | 5.62 | Mo(1a)···Mo(2) | 5.62 |
| Mo(1)···Mo(3) | 5.50 | Mo(1a)···Mo(3) | 5.50 |
| Mo(2)···Mo(2a) | 5.55 | Mo(3)···O(7) | 5.69 |
| Mo(1)···O(9a) | 5.77 | Mo(1a)···O(9) | 5.77 |
| Mo(2)···O(8a) | 6.06 | Mo(2a)···O(8) | 6.06 |
| Mo(1)···Mo(2) | 3.38 | Mo(1a)···Mo(2a) | 3.38 |
| Mo(2)···Mo(3) | 3.38 | Mo(2a)···Mo(3) | 3.38 |
| Mo(1)···Mo(1a) | 3.71 | | |
| O(10)···O(10a) | 3.14 | O(11)···O(11a) | 3.08 |
| O(12)···O(12a) | 4.48 | | |
| O(7)···O(8) | 3.70 | O(7)···O(8a) | 3.70 |
| O(8)···O(9) | 3.70 | O(8a)···O(9a) | 3.70 |
| O(9)···O(9a) | 3.64 | | |
| P(1)···O(7) | 3.35 | P(1a)···O(7a) | 3.35 |
| P(1)···O(8a) | 3.35 | P(1a)···O(8) | 3.35 |
| P(1)···O(8) | 4.02 | P(1a)···O(8a) | 4.02 |
| P(1)···O(9) | 3.04 | P(1a)···O(9a) | 3.04 |
| P(1)···O(9a) | 3.93 | P(1a)···O(9) | 3.93 |
| P(1)···Mo(1) | 3.62 | P(1a)···Mo(1a) | 3.62 |
| P(1)···Mo(2) | 3.44 | P(1a)···Mo(2a) | 3.44 |
| P(1)···Mo(3) | 3.48 | P(1a)···Mo(3) | 3.48 |
| P(1)···Mo(1a) | 3.31 | P(1a)···Mo(1) | 3.31 |
| P(1)···Mo(2a) | 3.54 | P(1a)···Mo(2) | 3.54 |

**Table 9** Bond angles used in CHARMm for polyoxomolybdate cages for terminal oxygens

| | Angle/° | | Angle/° |
|---|---|---|---|
| OA1–MO1–OA2 | 103.5 | OA1–MO1–OC3 | 172.0 |
| OA1–MO2–OA2 | 103.5 | OA1–MO2–OC2A | 90.0 |
| OA1–MO3–OA2 | 103.5 | OA1–MO2–OC2B | 90.0 |
| OA1–MO1–OB | 100.0 | OA2–MO2–OC3 | 90.0 |
| OA1–MO2–OB | 100.0 | OA2–MO2–OC2A | 162.5 |
| OA1–MO3–OB | 100.0 | OA2–MO2–OC2B | 162.5 |
| OA2–MO1–OB | 100.0 | OA1–MO2–OC3 | 162.5 |
| OA2–MO1–OB | 100.0 | OA1–MO3–OC2A | 87.0 |
| OA2–MO1–OB | 100.0 | OA2–MO3–OC2B | 87.0 |
| OA1–MO1–OC1 | 84.0 | OA1–MO3–OC2B | 168.0 |
| OA2–MO1–OC3 | 84.0 | OA2–MO3–OC2A | 168.0 |
| OA2–MO1–OC1 | 172.0 | | |

*Crystal Structures.*—The anions of conjugates **1**–**3** all lie on a unique crystallographic $C_2$ axis passing through Mo(3) and O(7). Their geometry is similar to that known for the $[(PO)_2Mo_5O_{21}]^{6-}$ anion, the so-called Strandberg[9] structure. It consists of a ring of five distorted $MoO_6$ octahedra and two $RPO_3$ tetrahedra. The distortion of the octahedra consists of the molybdenum atoms being displaced towards their two *cis* terminal oxygens. There are three crystallographically independent Mo atoms in each structure. The five $MoO_6$ octahedra are joined in the sequence Mo(1), Mo(2), Mo(3), Mo(2a), Mo(1a) by edge sharing of two oxygens (one oxo and one bonded also to phosphorus); the ring is completed and five-fold symmetry prevented by the sharing of only one oxygen, O(7), between Mo(1) and Mo(1a). The two $RPO_3$ tetrahedra cap the top and bottom of the ring, with one oxygen shared by only one $MoO_6$ octahedron (a corner-sharing one) and the other two edge-shared by two $MoO_6$ octahedra each. The Mo–O–Mo bond angles in the ten-membered Mo–O(oxo) ring reflect the different modes of linking the octahedra, the four edge-sharing angles being in the range 122–126° whereas the corner-sharing angles are 147–150° as observed for all of the Strandberg-type crystal structures.

Selected interatomic distances for the two anions are shown in Table 5. Further consensus distances used later for restraints

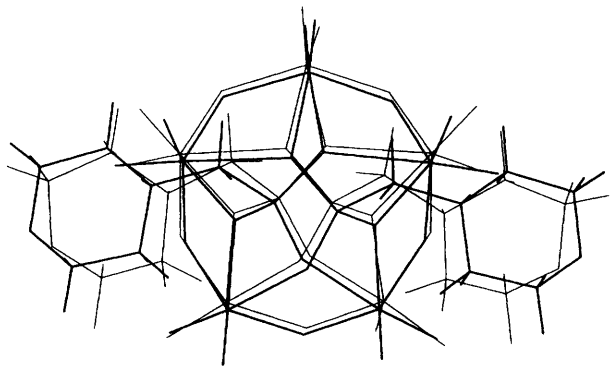

**Fig. 5** Superposition and fit of the minimised phosphonomolybdate geometry of conjugate **2** obtained using the force field, with that of the unminimised crystal structure

in modelling are shown in Tables 7 and 8. The Mo · · · Mo interatomic distances across the cage tend to be similar (as in the case of all the Strandberg-type structures studied), although the distances from Mo(1/1a) to Mo(2a/2) are slightly longer which is a result of the corner sharing of an oxygen by these molybdenums. The P · · · P interatomic distances are remarkably consistent, being within 0.01 Å of each other.

A prominent feature of all the anions is that of the two intramolecular hydrogen bonds within the structures. The heterocyclic rings bend over towards the molybdenum cage to form intramolecular hydrogen bonds to terminal molybdenum oxygens *via* the protonated nitrogen (Figs. 1 and 2). This is reflected in the terminal M=O bond lengths (Table 5); for the non-bonded types Mo–O ≈1.70 Å whereas for the hydrogen-bonded type the lengths are slightly longer, 1.72–1.74 Å.

The crystal packing for all three conjugates **1–3** shows common basic features, the most notable being the extensive intermolecular hydrogen bonding. This is illustrated in Fig. 3 for conjugate **3**. The large anions are in close contact with guanidinium cations and water molecules occupying relatively small interstices. The structures are held together by strong hydrogen bonding to guanidinium cations from the terminal and bridging oxygens in the clusters, with N–H · · · O distances of 2.1–2.4 Å, and by interactions between the ring hydrogens and the molybdenum oxygens. The guanidinium positions differ in each conjugate as a result of different hydrogen bonding. The water in the structures also forms hydrogen bonds to the oxygens in the molybdenum cluster, particularly with the terminal oxygens in the conjugate. There are three distinct types of terminal oxygens [O(1)–O(6)]: those unaffected by hydrogen-bonding Mo–O with lengths of ≈1.700 Å; those involved in hydrogen bonding to only one species with lengths of ≈1.710 Å; and those multiply hydrogen bonded with lengths of 1.720–1.740 Å. These effects are particularly well illustrated by O(5). This oxygen is involved in the intramolecular hydrogen bond with the protonated nitrogen of the appending heterocyclic ring in all three structures. In conjugate **1** it is hydrogen bonded solely to this nitrogen with a Mo–O length of 1.715 Å; however in conjugates **2** and **3** this is further elongated to 1.737 and 1.731 Å respectively by hydrogen bonding to water molecules [O–H · · · O(5) 1.966 and 2.090 Å respectively].

The bridging oxygens show a common trend in their bond lengths to Mo. In all edge-sharing cases the bond to one Mo is much longer than that to the other. This is a phenomenon observed in other polyoxometalate structures.[27] A clear effect of hydrogen bonding is noted for the corner-sharing oxygens O(7). In conjugate **1** the Mo–O length is 1.947 Å (hydrogen bond length 2.238 Å), in **2** it is 1.930 Å (hydrogen bond length 2.440 Å), and in **3** 1.917 Å (no hydrogen bond), *i.e.* the length increases as the hydrogen-bonding distance increases from 1.917 in **3** to 1.947 Å in **1**.

Noteworthy are the increased Mo–O bond lengths for O(10), O(11) and O(12), the oxygens which are bound to phosphorus. These long bonds from the phosphonate to the molybdenum cluster suggest that the molecule could be fluxional in solution, with the phosphonate groups readily exchangeable. Pope and co-workers[28] noted that in the tungsten analogue $[(PO)_2W_5O_{21}]^{6-}$ the $^{183}W$ NMR spectrum revealed a triplet-like signal ($^2J_{PW}$) which suggests a rapid exchange process, since a more complex coupling pattern to magnetically non-equivalent tungstens would be expected if the phosphate were stationary on the cluster.

**Table 10** Root-mean-square fits for minimised *vs.* X-ray crystal structures

| | r.m.s. | |
|---|---|---|
| Appending moiety R | For 18 cage atoms[a] | For 28 cage atoms[b] |
| Morpholino (**1**) | 0.046 | 0.059 |
| Thiomorpholino (**2**) | 0.056 | 0.065 |
| Piperidino (**3**) | 0.045 | 0.061 |
| Methyl 1[c] | 0.043 | 0.083 |
| Methyl 2[c] | 0.042 | 0.074 |
| Phenyl[d] | 0.061 | 0.080 |
| Aminoethyl | 0.091 | 0.140 |
| Oxygen | 0.042 | 0.100 |

[a] The 18 atoms are those involved in distance restraints, *i.e.* every cage atom except the terminal oxygens. [b] The 28 atoms are all the cage atoms including the terminal oxygens which were not involved in the distance restraints. [c] Two independent cages are present in the unit cell, possessing slightly different geometries. [d] Two optical isomers present in the unit cell; only one could be modelled using the restraints.

**Table 11** C–H · · · O Hydrogen bond distances (Å)

| | Oxygen atom | | | | | |
|---|---|---|---|---|---|---|
| Conjugate | O(2) | O(3) | O(4) | O(8) | O(9) | O(12) |
| **2** | | 2.435 | 2.369 | | 2.459 | 2.400 |
| **3** | 2.372 | | 2.396<br>2.263 | 2.378 | | 2.468 |

The second form of interaction between the anions, and perhaps the most significant, is that between the heterocyclic ring hydrogens and the molybdenum oxygens (Table 11). The CH protons of the ring and the $NCH_2P$ group are extremely close to the terminal Mo=O and bridging Mo–O–P oxygens on the adjacent anions. The C–H · · · O distances are in the range 2.3–2.5 Å suggesting that these may in fact be weak hydrogen bonds. Indeed C–H · · · O hydrogen bonding is not uncommon with water as acceptor group as recent reviews of neutron diffraction data[29,30] point out. In these reviews it is concluded that 'CH donors may participate in the co-ordination of water molecules in the same way and with the same functionality as OH and NH'. These observed distances in this work are much shorter than the average described for the 101 water molecules covered by the review[29] (in 46 crystal structures), where H · · · $O_w$ distances were most abundant in the range 2.7–3.0 Å and in fact only eight lengths of < 2.5 Å were noted.[29] A search of the Cambridge Structural Database[31] indicated this type of C–H · · · O=Mo hydrogen bonding may be a common feature, but it is explicitly noted only in two papers[32,33] where C–H · · · O=Mo distances < 2.5 Å are quoted.

*Comparison of Conjugates* **1–3** *with Related Structures.*— Only five other examples of Strandberg-type structures $[(RP)_2Mo_5O_{21}]^{4-}$ have been solved which contain the phosphorus heteroatom: these are the original $[(PO)_2Mo_5O_{21}]^{6-}$ anion solved by Strandberg[9] and others using different counter ions;[34–36] $[(MeP)_2Mo_5O_{21}]^{4-}$ the methylphosphonate conjugate;[10] $[(PhP)_2Mo_5O_{21}]^{4-}$ the phenylphosphonate

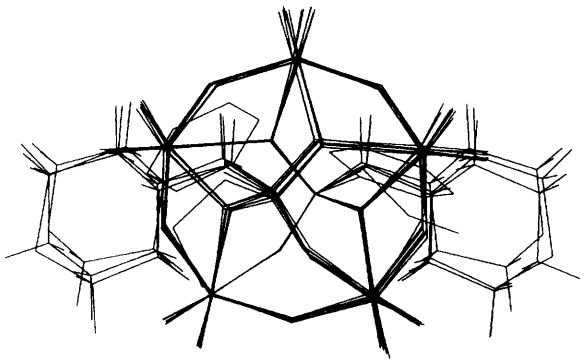

**Fig. 6** Superposition of the seven pentamolybdodiphosphonato-containing crystal structures

conjugate;[11] $[(H_3NCH_2CH_2P)_2Mo_5O_{21}]^{2-}$ the aminoethylphosphonate conjugate;[12] the $[H(PO)_2Mo_5O_{21}]^{5-}$ anion[37] and the $[\{O(CH_2CH_2)_2NHCH_2P\}_2Mo_5O_{21}]^{2-}$ anion.[6] Other pentamolybdate structures with different heteroatoms have also been reported: $[(SO)_2Mo_5O_{21}]^{6-}$ the sulfate conjugate;[38] $[S_2Mo_5O_{21}]^{4-}$ the sulfite conjugate;[39] $[(CH_2CHCH_2As)_2Mo_5O_{21}]^{4-}$ the allylarsenate conjugate;[40] and $[(Pr^nAs)_2Mo_5O_{21}]^{4-}$ the propylarsenate conjugate.[41] The superposition of the seven phosphorus-containing structures is shown in Fig. 6. It is evident that very little deviation is seen in the basic structure of the heteropolymolybdate anion $[(RP)_2Mo_5O_{21}]^{n-}$. The first bonds leading out from the heteroatom (*i.e.* organic groups or oxygen) all radiate to a similar position preserving the near-tetrahedral geometry of the heteroatom. It is from this first bond that the structures then deviate significantly, with the various organic moieties occupying different positions for preferred steric and electrostatic reasons, *e.g.* the intramolecular hydrogen bond from the protonated nitrogen in the aminomethylphosphonic acids (conjugates **1–3**) dictates the lie of the organic group.

Since polyoxomolybdate cages are frequently implicated in catalysis, and it seemed that the cage in our conjugates had a well defined geometry, we considered a force-field approach to the structure which could then be used as a novel model for a catalytic surface. Early molecular-mechanics force fields were developed to deal with organic molecules and rely heavily on the two-centre bond convention. Extension to metal ions followed. Recent reviews survey the application of molecular mechanics to metal complexes.[42,43] However, the molybdenum conjugates in this paper are not conventional co-ordination compounds. Three different molybdenum atom types and seven different oxygen types are required in the force field (see Table 6), while the number of distinct angle, torsion and improper torsion terms for the CHARMm force field would be large. Recognising that in later studies of macrocycles and other organic moieties attached to the molybdenum cage only the electrostatic, hydrogen bonding and van der Waals interactions with the cage would be important, it should suffice to model the cage skeletal geometry using flexible distance restraints. The approach we used is similar to the central force-field concept used by Saunders and Jarret[44] which involves only a force along the line joining two atoms. It should be recognised that both the molecular-mechanics and distance restraints methods are based on highly artificial models of a molecule: they are valid only in so far as they reproduce the required features of the model, in this case the cage geometry.

We have recently[22] used distance restraints in a force field to model *o*-carborane cage geometry. Superficially the polyoxomolybdate cage presents a similar problem, in that each Mo is six-co-ordinate and appears to be part of a cage. As a preliminary approach we used distance restraints around the atoms of the ring to hold the molecule in place. In the enclosed cage structure of carborane, where each atom has a connectivity of six, forces along the bond directions were adequate to hold the cage rigid. In the mixed cage presented here, while Mo atoms are six-connected, the oxygens of the cage may be two- or three-connected. In preliminary minimisations with interbond restraints alone the cage deformed drastically. To circumvent this, additional restraints were set up between non-bonded atoms and especially involving oxygens (see Table 8). The crystal structures of the two phosphonomolybdate anions of **2** and **3** look almost identical (Figs. 1 and 2): they are shown superimposed (together with the other structures) about the cage atoms in Fig. 6. It is clear that the basic structure of the molybdenum–oxygen cage is almost identical in all of these conjugates. It thus seemed important to produce a force-field representation of the cages for inclusion in future molecular-modelling work.

*Modelling of Polyoxometalate Cage.*—The force-field representation of the cage described gave a reasonable geometric fit to the crystal structures reported in this paper and to others taken from the literature, with root-mean-square (r.m.s.) deviations for the cage atoms as shown in Table 10. In further considerations of the geometry of the cage-derivatised macrocycles, the cage should influence the geometry of the macrocycle mainly through electrostatic, van der Waals and hydrogen-bonding interactions, and through the torsions of the single C–P bond by which the organic group is attached. Thus the present model is adequate to consider the effect of conjugation on the macrocycle. The most important feature would seem to be the charge on the molybdate surface: the oxygens are relatively nucleophilic and, as shown in our survey of structures in the database, are commonly found within hydrogen-bonding distance of aliphatic H–C bonds in the vicinity. This feature may well be important in activation of the organic moiety in the catalytic activity of polyoxometalates.

*Infrared Analysis of Conjugates* **2–6**.—The phosphonomolybdate conjugates show a range of well defined stretching vibrations. The Mo–O stretching vibration is very well defined[3,27] as two very intense, slightly broad bands in the range 950–880 $cm^{-1}$ which correspond to the terminal Mo=O bonds and a broader stretching vibration is observed at a lower range of 700–680 $cm^{-1}$ which corresponds to the bridging Mo–O–Mo bonds. Several other well defined stretching and bending frequencies can be observed. Starting at higher frequencies, the strong $\nu_{def}(NH^+)$ is seen as a large band for the guanidinium cation (1660–1650 $cm^{-1}$) and as a weaker band close to this at 1630–1560 $cm^{-1}$ for $\nu_{def}(PCH_2NH^+)$. Following these bands are fairly weak $\nu_{def}(CH_2)$ bending signals of which three or four are usually noted around 1480–1400 $cm^{-1}$. Close to these are the $\nu_{str}(PC)$ stretching vibrations at 1300–1220 $cm^{-1}$ which occur as fairly weak but very sharp signals. The final noteworthy signal is the weak $\nu_{def}(PC)$ bending at $\approx$770 $cm^{-1}$. The conjugates investigated all show similar IR spectra which are roughly superimposable: this assists identification of the conjugates. The various signals are in Table 12.

## Conclusion

An important feature of the crystal structure of the conjugates is the formation of an intramolecular hydrogen bond from the protonated nitrogen of the aminomethylphosphonic acid to one of the terminal oxygens attached to molybdenum. This has the effect of bending over the appended ligand towards this metal–oxygen surface: it offers the possibility of bringing a second metal atom bound in the macrocyclic cavity in close contact with the surface of the conjugate. A variety of metals could be introduced in this manner, from hard alkali metals (*via* oxygen crowns) to soft thiophiles (*via* sulfur crowns). Further work will continue to explore these possibilities, especially the formation of crown thioether conjugates, since dual-functionality catalysts

**Table 12** Infrared stretching and deformation bands ($cm^{-1}$) for conjugates **2–6**

| Conjugate | $CH_{2\ def}$ | $\nu_{str}(PC)$ | $\nu_{str}(PO)$ | $\nu_{str}(MoO_t)$ | $PC_{def}$ | $\nu_{str}(MoO_b)$ |
|---|---|---|---|---|---|---|
| **2** | 1453, 1414 | 1289, 1250 | 1140, 1065, 981 | 930, 899 | 768 | 687 |
| **3** | 1472, 1455, 1431, 1408 | 1271, 1223 | 1151, 1132, 1060, 985 | 939, 910 | 768 | 696 |
| **4** | 1460, 1443, 1433, 1410 | 1300, 1261 | 1143, 1124, 1064, 978 | 943, 922 | 772 | 694 |
| **5** | 1455, 1428 | 1289, 1250 | 1145, 1136, 1070, 987 | 932, 916 | 772 | 683 |
| **6** | 1455, 1431, 1408 | 1296, 1260 | 1138, 1063, 979 | 937, 910 | 768 | 694 |

are in great demand. Attempts to solubilise the cages in organic solvents are also underway. The bringing together of these two major research areas could prove beneficial to both the macrocyclic and polyoxometalate chemist in the pursuit of supramolecular chemistry.

On superimposing the seven known cage structures the only significant variation found is in the appended organic moiety. The geometries of the central cluster can be regarded as fixed, thus allowing them to be modelled with a central force field. A force-field representation for the cages has been developed which models the known cages with sufficient accuracy to reproduce the crystal geometries: this may be useful for future modelling of catalytic function.

## Acknowledgements

The authors are grateful for support from the EPSRC and Courtaulds Coatings plc. We would also like to acknowledge the use of the EPSRC-funded Chemical Database Service.

## References

1 H. Reuter, *Angew. Chem., Int. Ed. Engl.*, 1992, **31**, 1185.
2 J. Berzelius, *Ann. Phys. (Leipzig)*, 1826, **6**, 369.
3 W. Kwak, M. T. Pope and T. F. Scully, *J. Am. Chem. Soc.*, 1975, **97**, 5735.
4 A. Yagasaki, I. Andersson and L. Pettersson, *Inorg. Chem.*, 1987, **26**, 3926.
5 W. Kwak, M. T. Pope and P. R. Sethuraman, *Inorg. Synth.*, 1990, **27**, 123.
6 M. P. Lowe, J. C. Lockhart, W. Clegg and K. A. Fraser, *Angew. Chem., Int. Ed. Engl.*, 1994, **33**, 451.
7 L. Pettersson, I. Andersson and L.-O. Öhman, *Inorg. Chem.*, 1986, **25**, 4726.
8 L. Pettersson, I. Andersson and L.-O. Öhman, *Acta Chem. Scand., Ser. A*, 1985, **39**, 53.
9 R. Strandberg, *Acta Chem. Scand., Ser. A*, 1973, **27**, 1004.
10 J. K. Stalick and C. O. Quicksall, *Inorg. Chem.*, 1976, **15**, 1577.
11 D.-G. Lyxell and R. Strandberg, *Acta Crystallogr., Sect. C*, 1988, **44**, 1535.
12 D.-G. Lyxell, R. Strandberg, D. Boström and L. Pettersson, *Acta Chem. Scand., Ser. A*, 1991, **45**, 681.
13 C. Seel and F. Vögtle, *Angew. Chem., Int. Ed. Engl.*, 1992, **31**, 528.
14 *Frontiers in Supramolecular Organic Chemistry and Photochemistry*, eds. H.-J. Schneider and H. Dürr, VCH, Weinheim, 1990.
15 J.-M. Lehn, *Angew. Chem., Int. Ed. Engl.*, 1990, **29**, 1304.
16 A. Proust, P. Gouzerh and F. Robert, *Angew. Chem., Int. Ed. Engl.*, 1993, **32**, 115.
17 V. W. Day and W. G. Klemperer, *Science*, 1985, **228**, 533.
18 M. T. Pope and A. Müller, *Angew. Chem., Int. Ed. Engl.*, 1991, **30**, 34.
19 J. Cosier and A. M. Glazer, *J. Appl. Crystallogr.*, 1986, **19**, 105.
20 W. Clegg, *Acta Crystallogr., Sect. A*, 1981, **37**, 22.
21 G. M. Sheldrick, *SHELXTL/PC Users' manual*, Siemens Analytical X-Ray Instruments, Madison, WI, 1990, SHELXL 93, program for crystal structure refinement, University of Göttingen, 1993.
22 J. D. Holbrey, P. B. Iveson, J. C. Lockhart, N. P. Tomkinson, F. Teixidor, A. Romerosa, C. Vinas and J. Rius, *J. Chem. Soc., Dalton Trans.*, 1993, 1451.
23 QUANTA 3.0, Polygen Corporation, 1986, 1990.
24 CHARMm, B. R. Brooks, R. E. Bruccoleri, B. D. Olafson, D. J. States, S. Swaminathan and M. Karplus, *J. Comput. Chem.*, 1983, **4**, 187.
25 F. H. Allen, O. Kennard and R. Taylor, *Acc. Chem. Res.*, 1983, **16**, 146.
26 J. Mestres, M. Duran, P. Martín-Zarza, E. Medina de la Rosa and P. Gili, *Inorg. Chem.*, 1993, **32**, 4708.
27 M. T. Pope, *Prog. Inorg. Chem.*, 1991, **39**, 181.
28 P. R. Sethuraman, M. A. Leparulo, M. T. Pope, F. Zonnevijlle, C. Brévard and J. Lemerle, *J. Am. Chem. Soc.*, 1981, **103**, 7665.
29 T. Seiner and W. Saenger, *J. Am. Chem. Soc.*, 1993, **115**, 4540.
30 G. R. Desiraju, *Acc. Chem. Res.*, 1991, **24**, 290.
31 F. H. Allen, J. E. Davies, J. J. Galloy, O. Johnson, O. Kennard, C. F. Macrae, E. M. Mitchell, G. F. Mitchell, J. M. Smith and D. G. Watson, *J. Chem. Inf. Comput. Sci.*, 1991, **31**, 187.
32 Y. Do, X.-Z. You, C. Zhang, Y. Ozawa and K. Isobe, *J. Am. Chem. Soc.*, 1991, **113**, 5892.
33 E. M. McCarron and R. L. Harlow, *J. Am. Chem. Soc.*, 1983, **105**, 6178.
34 D.-G. Lyxell, R. Strandberg, D. Boström and L. Pettersson, *Acta Chem. Scand., Ser. A*, 1991, **45**, 681.
35 B. Hedmann, *Acta Crystallogr., Sect. B*, 1977, **33**, 3083.
36 J. Fischer, L. Richard and P. Toledano, *J. Chem. Soc., Dalton Trans.*, 1974, 941.
37 E. K. Andersen and J. Villadsen, *Acta Chem. Scand.*, 1993, **47**, 748.
38 T. Hori, S. Himeno and O. Tamada, *J. Chem. Soc., Dalton Trans.*, 1992, 275.
39 K. Y. Matsumoto, M. Kato and Y. Sasaki, *Bull. Chem. Soc. Jpn.*, 1976, **49**, 106.
40 Y.-T. Ku, B.-Y. Liu and X. Wang, *Inorg. Chim. Acta*, 1989, **161**, 233.
41 B.-Y. Liu, Y.-T. Ku, M. Wang and P.-J. Zheng, *Inorg. Chem.*, 1988, **27**, 3868.
42 P. Comba, *Coord. Chem. Rev.*, 1993, **123**, 1.
43 B. P. Hay, *Coord. Chem. Rev.*, 1993, **126**, 177.
44 M. Saunders and R. M. Jarret, *J. Comput. Chem.*, 1986, **7**, 578.

*Received* 26*th May* 1994; *Paper* 4/03149K